Mathematical Biosciences and Engineering

https://www.aimspress.com/journal/mbe

MBE, 23(2): 449–473.
DOI: 10.3934/mbe.2026018
Received: 10 November 2025
Revised: 15 December 2025
Accepted: 23 December 2025
Published: 07 January 2026

Research article

Stability and bifurcation of difference equations from stochastic logistic models

Haiyan Wang[1,*] **and Emily Wang**[2]

[1] School of Mathematical and Natural Sciences, Arizona State University, Phoenix, AZ 85069, USA
[2] LinkedIn, San Francisco, CA 94105, USA

* **Correspondence:** Email: haiyan.wang@asu.edu.

Abstract: This paper investigates the stochastic logistic difference equation, $X_{n+1} = rX_n(1 - X_n)\varepsilon_n$, where X_n is a random variable of population size, and $\{\varepsilon_n\}$ represents independent random perturbations with $E[\varepsilon_n] = 1$ and $E[\varepsilon_n^2] = v > 1$. Under the Gaussian moment-closure approximation, we derived a closed system of difference equations for the mean and variance of X_n. The analysis of the system of difference equations identified two classes of equilibria: a trivial equilibrium $(0, 0)$ representing extinction, and nontrivial equilibria corresponding to positive steady population levels. Explicit conditions for the existence and local stability of these equilibria were obtained, showing that the extinction state is stable when $r^2v < 1$, whereas nontrivial equilibria arise for $r > 1$ with stability dependent on the stochastic intensity v. The saddle-node (fold) bifurcation induced by variations in the stochastic intensity v was explicitly formulated. Monte Carlo simulations confirmed the analytical analysis.

Keywords: logistic difference equation; stochastic population equations; Gaussian moment-closure approximation; equilibrium; stability; bifurcation

1. Introduction

The logistic difference equation is a fundamental model in ecology and applied mathematics, used to describe the dynamics of population growth in environments with finite resources. It captures the essential interplay between a population's growth potential and the limitations imposed by its environment, making it a powerful tool for studying nonlinear dynamics in ecological and other resource-constrained systems.

In their deterministic form, these models capture an initial phase of exponential expansion that gradually slows as the population approaches the carrying capacity, the maximum number of individuals that the environment can sustain. The behavior of the logistic model is highly sensitive to

the intrinsic growth rate, which determines the speed of population increase and governs transitions between stability, oscillation, and chaotic dynamics [1–4]. Because of their simplicity and rich dynamic structure, deterministic logistic equations have become fundamental tools for studying nonlinear population dynamics and resource-limited ecological systems.

Stochastic extensions of the logistic model significantly enhance the deterministic framework by accounting for the unpredictable nature of real-world ecosystems. Unlike deterministic models, which predict a single, fixed trajectory based on starting conditions, stochastic models capture a range of possible population outcomes, revealing both the average trend and the uncertainty around it. By incorporating random environmental fluctuations, such as shifts in climate, resource availability, or unexpected disturbances, these models offer a more realistic picture of how populations evolve in dynamic, uncertain settings. This makes them especially valuable for studying ecosystems affected by irregular conditions, like variable weather patterns or resource instability. As a result, research into stochastic logistic models, both in discrete and continuous forms, has become a dynamic field, with extensive studies exploring their behavior and practical implications for understanding ecological systems and guiding conservation efforts [3–8].

Quantitative analysis of stochastic difference equations often relies on moment-closure methods, which approximate the evolution of a system's statistical moments through a finite set of recursive equations. In this approach, expectations are taken over the stochastic updates to obtain relations for the mean and variance, while higher-order moments are expressed in terms of these lower ones under the assumption of approximate distributions. This closure transforms inherently stochastic dynamics into a deterministic system describing the evolution of the mean and variance, thereby avoiding the need to track individual realizations. The Gaussian moment closure provides an efficient analytical framework for investigating nonlinear, noise-driven discrete-time systems, such as stochastic logistic models, and facilitating studies of stability, bifurcation, and long-term population behavior while preserving the influence of environmental variability [5, 9–13].

Our focus in this paper is the dynamics of the derived system of difference equations for the mean and variance of X_n obtained directly from

$$X_{n+1} = rX_n(1 - X_n)\varepsilon_n,\ n = 1, 2, ..., \tag{1.1}$$

where X_n is a random variable representing a population size at time n, $r > 0$ is a constant representing the intrinsic growth rate, and ε_n is a random variable accounting for stochastic perturbations, independent of X_n, with

$$E[\varepsilon_n] = 1,\ E[\varepsilon_n^2] = v > 1.$$

We show that this moment system under the Gaussian moment-closure approximation admits two types of equilibria: the trivial equilibrium $(\mu^*, s^*) = (0, 0)$, and one or two nontrivial equilibria $(\mu^*, s^*) > 0$, corresponding to sustainable positive population levels. The stability analysis reveals that the trivial equilibrium is locally asymptotically stable when $r^2 v < 1$, a condition under which small populations inevitably decline to extinction. When $r > 1$, the system gives rise to nontrivial equilibria whose stability depends on the interaction between the intrinsic growth rate r and the stochastic intensity $v = E[\varepsilon_n^2]$. For moderate values of v, a stable nontrivial equilibrium emerges, ensuring long-term persistence at a positive mean population level, whereas large stochastic perturbations or high growth rates can destabilize the equilibrium, leading to fluctuations or collapse. The study also includes the

analysis of the saddle-node (fold) bifurcation that emerges as the stochastic intensity v varies. These results provide a unified theoretical framework linking the parameters of the stochastic logistic model to population persistence, extinction, and the stabilizing influence of environmental variability.

The study continues the work in [14, 15] where the authors investigated the relations between the parameters in (1.1) and the transitions from steady states to chaos in the stochastic models with the gamma distribution [16]. The key new contributions of this paper include: 1) the development of a system of difference equations for the mean and variance of X_n obtained directly from (1.1) under the Gaussian moment-closure approximation, establishing a moment-based framework for analyzing stochastic logistic dynamics; 2) the derivation of explicit analytical expressions for the equilibrium conditions and stability criteria of both trivial and nontrivial equilibria under the Gaussian moment-closure approximation, as well as analysis of how changes in the stochastic intensity v give rise to a saddle-node (fold) bifurcation in the system; and 3) a comprehensive investigation of the effects of stochastic perturbations and distributional parameters on the intrinsic growth rate and population persistence, providing new biological insights into how environmental variability shapes population stability and extinction risk.

The remainder of this paper is organized as follows. Section 1 provides an introduction to the logistic difference equation and its stochastic extensions, highlighting the motivation, results, and significance of this study. In Section 2, under the Gaussian moment-closure approximation, we derive a system of difference equations for the first and second moments of X_n directly from the stochastic logistic equation (1.1), establishing the analytical foundation for the subsequent stability analysis. Section 3 examines the trivial equilibrium $(\mu^*, s^*) = (0, 0)$, representing population extinction, and presents the conditions under which this equilibrium is locally asymptotically stable. Section 4 focuses on the existence and stability of nontrivial equilibria $(\mu^*, s^*) > 0$, corresponding to sustainable population levels, and explores how the parameters r and v influence their stability and bifurcations. Finally, Section 5 discusses the biological implications of the stability results, compares the analytical findings with Monte Carlo simulations, and summarizes the broader significance of the study in understanding population persistence and extinction under stochastic environments.

2. Gaussian moment–closure and difference equations

The stochastic process $X_{n+1} = rX_n(1 - X_n)\varepsilon_n$ forms a Markov chain as each ε_n is independent of the past. The Markov property allows the moment hierarchy to be written in recursive form. Moment closure is a prevalent method to study nonlinear stochastic differential equations. To obtain a closed system of equations for the first few moments, it is common to invoke a Gaussian moment-closure approximation, assuming that fluctuations around the mean are approximately normal. This approximation is justified when stochastic perturbations are small and the process remains near its deterministic trajectory. Thus, while the Markov property enables the recursive moment formulation, the Gaussian closure provides an analytically tractable approximation for solving it [5, 9–13, 17].

In particular, [10] provided theoretical justification for using a Gaussian moment-closure approximation in stochastic population differential equations. They demonstrated that population growth governed by nonlinear logistic-type dynamics can be described as a Markovian jump process whose moment equations are unclosed, since lower-order moments depend on higher-order ones. To address this, they tested several standard moment-closure approximations, including the normal

(Gaussian) closure, which expresses higher moments as functions of the first two moments. They find that Gaussian or normal-type closures substantially improve predictions of stochastic dynamics compared to purely deterministic descriptions by incorporating variance effects in a tractable way. Thus, their analysis supports the adoption of Gaussian moment assumptions as an effective second-order approximation for nonlinear stochastic difference equations as well.

The stochastic logistic model (1.1) with random perturbations ε_n generates fluctuations around the deterministic trajectory due to the small independent random perturbation in each iteration. To obtain a tractable system for the stochastic difference equations, we adopt the Gaussian moment-closure approximation. This approach does not assume that X_n itself is normally distributed, but rather that its first few moments satisfy the same relationships as those of a Gaussian random variable. Specifically, we assume that the moments of $X_n, n = 1, 2, ...,$ satisfy

$$\begin{aligned} &E[X_n] = \mu_n, && E[X_n^2] = \mu_n^2 + \sigma_n^2, \\ &E[X_n^3] = \mu_n^3 + 3\mu_n\sigma_n^2, && E[X_n^4] = \mu_n^4 + 6\mu_n^2\sigma_n^2 + 3\sigma_n^4, \end{aligned} \tag{2.1}$$

with $\mu_n, \sigma_n > 0$. The Gaussian moment-closure approximation closes the infinite hierarchy of moment equations and allows use to derive consistency conditions to preserve the nonnegativity of the mean of X_n for biological feasibility. If a random variable X follows a normal distribution, it satisfies the relation (2.1) [18] or from the Appendix at the end of [15].

We now derive a system of difference equation for the first and second moments of X_n directly from (1.1).

Theorem 2.1. *Consider the stochastic logistic difference equation* (1.1)*. Suppose that ε_n is any random variable and independent of X_n with*

$$E[\varepsilon_n] = 1, \ E[\varepsilon_n^2] = v > 1.$$

Assume that X_n satisfies the Gaussian moment-closure approximation (2.1)*. Defining*

$$\mu_{n+1} = E[X_{n+1}], \ s_{n+1} = \sigma_{n+1}^2 = \mathrm{Var}[X_{n+1}],$$

we obtain the following system of difference equations:

$$\mu_{n+1} = F_1(\mu_n, s_n), \tag{2.2}$$

$$s_{n+1} = F_2(\mu_n, s_n), \tag{2.3}$$

where

$$F_1(\mu, s) = r(\mu - \mu^2 - s)$$

and

$$F_2(\mu, s) = r^2 v(\mu^4 - 2\mu^3 + \mu^2 + 6\mu^2 s - 6\mu s + s + 3s^2) - r^2(\mu - \mu^2 - s)^2.$$

Proof. From (1.1), the first moment of X_{n+1} is given by

$$E[X_{n+1}] = rE[X_n(1 - X_n)] = r(\mu_n - \mu_n^2 - \sigma_n^2) \tag{2.4}$$

and the second moment of X_{n+1} is

$$E[X_{n+1}^2] = r^2 v E[X_n^2(1 - X_n)^2] = r^2 v E[X_n^2 - 2X_n^3 + X_n^4].$$

It follows that

$$\begin{aligned} E[X_{n+1}^2] &= r^2 v E[X_n^2(1 - X_n)^2] \\ &= r^2 v(\mu_n^4 - 2\mu_n^3 + \mu_n^2 + 6\mu_n^2\sigma_n^2 - 6\mu_n\sigma_n^2 + \sigma_n^2 + 3\sigma_n^4). \end{aligned} \tag{2.5}$$

Finally, $\mathrm{Var}[X_{n+1}] = E[X_{n+1}^2] - (E[X_{n+1}])^2$ gives

$$\mu_{n+1} = r(\mu_n - \mu_n^2 - \sigma_n^2), \tag{2.6}$$

$$\sigma_{n+1}^2 = r^2 v(\mu_n^4 - 2\mu_n^3 + \mu_n^2 + 6\mu_n^2\sigma_n^2 - 6\mu_n\sigma_n^2 + \sigma_n^2 + 3\sigma_n^4) - r^2(\mu_n - \mu_n^2 - \sigma_n^2)^2. \tag{2.7}$$

Letting $s_n = \sigma_n^2$ completes the proof. □

Theorem 2.1 provides a general framework for analyzing the mean and variance of stochastic populations. The system (2.6)–(2.7) captures the nonlinear interaction between the mean population level μ_n and its dispersion σ_n^2 under random perturbations. The parameters r and v jointly determine how strongly stochasticity influences both the expected growth and the spread of the population size. In the deterministic limit $v = 1$ and $\sigma_n^2 \to 0$, the system approximately reduces to the classical logistic map

$$\mu_{n+1} = r\mu_n(1 - \mu_n).$$

3. Trivial equilibrium

3.1. Stability analysis of trivial equilibrium

In this section, we analyze the equilibria of the trivial equilibrium system of difference equations (2.2)–(2.3), where $r > 0$ is the intrinsic growth parameter and $v = E[\varepsilon_n^2] > 1$ represents the stochastic intensity of the perturbation ε_n. The local stability of each equilibrium is determined by the eigenvalues of the Jacobian matrix evaluated at that equilibrium point. If all eigenvalues lie inside the unit circle, the equilibrium is locally asymptotically stable [3, 19].

Theorem 3.1 (Trivial equilibrium and local stability)**.** *The system* (2.2)–(2.3) *always admits the equilibrium*

$$(\mu^*, s^*) = (0, 0),$$

corresponding to the extinction state of the population. Under the assumptions of Theorem 2.1, the equilibrium $(0, 0)$ *is locally asymptotically stable if and only if*

$$r^2 v < 1.$$

Proof. Substituting $(\mu_n, s_n) = (0, 0)$ into (2.2)–(2.3), we find that $\mu_{n+1} = 0$ and $s_{n+1} = 0$, establishing that $(0, 0)$ is an equilibrium for any $r, v > 0$. Now we compute the Jacobian $J(\mu, s) = DF(\mu, s)$, where

$$F(\mu, s) = \begin{pmatrix} F_1 \\ F_2 \end{pmatrix}.$$

We compute the partial derivatives of F_1 and F_2. For $F_1(\mu, s) = r(\mu - \mu^2 - s)$,

$$\frac{\partial F_1}{\partial \mu} = r(1 - 2\mu), \qquad \frac{\partial F_1}{\partial s} = -r.$$

For $F_2(\mu, s) = r^2 v\, A(\mu, s) - r^2 B(\mu, s)$, where

$$A(\mu, s) = \mu^4 - 2\mu^3 + \mu^2 + 6\mu^2 s - 6\mu s + s + 3s^2, \qquad B(\mu, s) = (\mu - \mu^2 - s)^2,$$

we have (by direct differentiation)

$$\frac{\partial A}{\partial \mu} = 4\mu^3 - 6\mu^2 + 2\mu + 12\mu s - 6s, \qquad \frac{\partial A}{\partial s} = 6\mu^2 - 6\mu + 1 + 6s,$$

and

$$\frac{\partial B}{\partial \mu} = 2(\mu - \mu^2 - s)(1 - 2\mu), \qquad \frac{\partial B}{\partial s} = 2(\mu - \mu^2 - s)(-1).$$

Therefore

$$\frac{\partial F_2}{\partial \mu} = r^2 v \frac{\partial A}{\partial \mu} - r^2 \frac{\partial B}{\partial \mu}, \qquad \frac{\partial F_2}{\partial s} = r^2 v \frac{\partial A}{\partial s} - r^2 \frac{\partial B}{\partial s}.$$

We now evaluate the Jacobian at $(0, 0)$ by substituting $\mu = 0$, $s = 0$ into the partials computed above:

$$\left.\frac{\partial F_1}{\partial \mu}\right|_{(0,0)} = r, \quad \left.\frac{\partial F_1}{\partial s}\right|_{(0,0)} = -r,$$

and

$$\left.\frac{\partial F_2}{\partial \mu}\right|_{(0,0)} = r^2 v \cdot 0 - r^2 \cdot 0 = 0, \qquad \left.\frac{\partial F_2}{\partial s}\right|_{(0,0)} = r^2 v \cdot 1 - r^2 \cdot 0 = r^2 v.$$

Thus the Jacobian at $(0, 0)$ is the upper triangular matrix

$$J(0, 0) = \begin{pmatrix} r & -r \\ 0 & r^2 v \end{pmatrix}.$$

Because $J(0, 0)$ is triangular, its eigenvalues are the diagonal entries:

$$\lambda_1 = r, \qquad \lambda_2 = r^2 v.$$

The standard discrete-time linearization theorem ([19]) implies that the sufficient and necessary conditions such that the equilibrium $(0, 0)$ is locally asymptotically stable is

$$r < 1 \quad \text{and} \quad r^2 v < 1.$$

For $v > 1$, $r^2 v < 1$ implies $r < 1$ and therefore only $r^2 v < 1$ is needed. This completes the proof. □

The equilibrium $(0, 0)$ represents complete extinction, a degenerate population distribution centered at zero with vanishing variance. For small r and weak noise ($v \approx 1$), the stability conditions are satisfied, and the population mean and variance decay to zero exponentially. When $r > 1$, this equilibrium becomes unstable and the population either diverges or oscillates due to stochastic amplification.

3.2. *Monte Carlo simulations*

Figure 1 displays the temporal evolution of the sample mean and variance obtained from Monte Carlo simulations together with the corresponding analytic results from the moment-map equations for two small growth rates, $r = 0.1$ and $v = 1.05$. The trajectory of the mean and variance rapidly decays toward zero, indicating convergence to the trivial equilibrium $(\mu^*, \sigma^{2*}) = (0, 0)$. The close agreement between the moment-map predictions and the Monte Carlo ensemble averages confirms the accuracy of the Gaussian moment-closure approximation in this weakly nonlinear system. Because r is small, the local stability condition $r^2 v < 1$ is satisfied, and the stochastic perturbation ε_n has only a minimal effect on the dynamics. Consequently, both the deterministic and stochastic trajectories remain near the origin and quickly stabilize, exhibiting nearly identical behavior. These results demonstrate that, when the intrinsic growth rate is small, the system is strongly attracted to the extinction state and the influence of random fluctuations is negligible, leading to perfect consistency between analytic and Monte Carlo solutions.

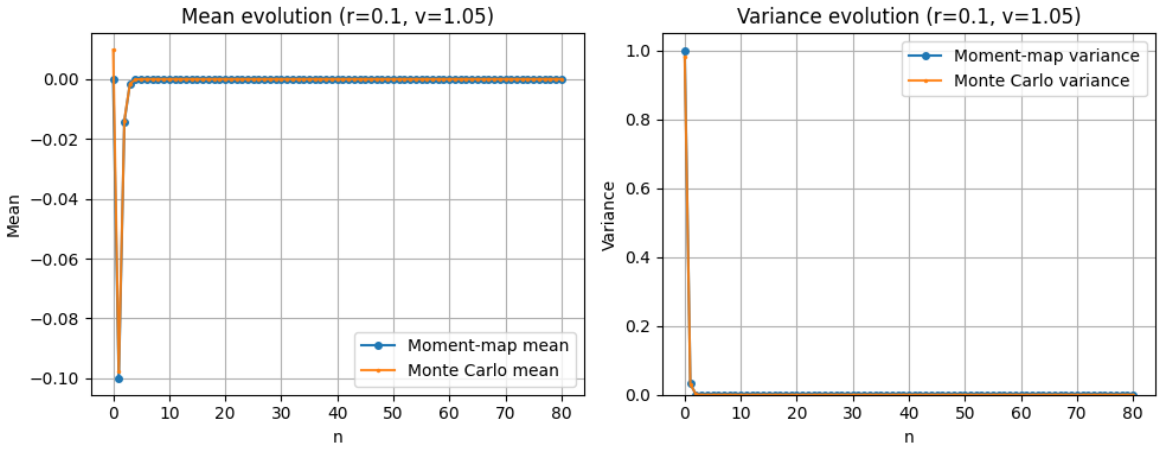

Figure 1. Simulated trajectories of μ_n and s_n converging to $(0, 0)$ for $r = 0.1$, $v = 1.05$.

From a biological perspective, the stability of the trivial equilibrium $(\mu^*, \sigma^{2*}) = (0, 0)$ corresponds to the extinction state of the population. When this equilibrium is locally asymptotically stable, small populations subjected to environmental fluctuations inevitably decline to zero over time, regardless of random perturbations, implying that the intrinsic growth rate r is insufficient to sustain persistence. The analytical stability condition $r^2 v < 1$ thus defines the parameter region in which extinction is inevitable, even in the presence of mild stochastic variability. In this regime, the effects of random environmental noise do not generate recovery but rather may accelerate convergence toward extinction by amplifying the effective damping around the zero state. Conversely, when the trivial equilibrium becomes unstable, the population can escape extinction and approach a positive nontrivial steady state, marking the transition from extinction risk to sustainable growth. Therefore, the stability of the trivial equilibrium provides a quantitative threshold for the persistence or collapse of a biological population under stochastic environmental perturbations.

4. Nontrivial equilibria

4.1. Existence of nontrivial equilibria

Theorem 4.1 (Existence of nontrivial equilibria)**.** *Under the assumptions of Theorem 2.1, and assume that $r > 1$. Then any nontrivial positive equilibrium ($\mu^* > 0, s^* > 0$) of* (2.2)–(2.3) *must satisfy*

$$s^* = \mu^*\Big(1 - \frac{1}{r} - \mu^*\Big), \tag{4.1}$$

$$P(\mu^*; r, v) := 2r^3v\mu^{*3} - 4r^3v\mu^{*2} + (3r^3v - 3rv)\mu^* - r^3v + r^2v + r - 1 = 0. \tag{4.2}$$

A positive root μ^* of (4.2) *corresponds to a positive feasible equilibrium ($\mu^* > 0, s^* > 0$) if*

$$0 < \mu^* \le 1 - \frac{1}{r}.$$

In addition, $P(\mu^*; r, v)$ has no feasible solution for $r \ge 3$.

Remark 4.2. The trivial solution $(0, 0)$ always exists. In the proof of Theorem 4.1, we assume $\mu^* > 0$, and in addition, because of the assumption that $r > 1$, then $r^2v > 1$ and

$$P(0; r, v) = -r^3v + r^2v + r - 1 \tag{4.3}$$

$$= (r - 1)(1 - r^2v) < 0. \tag{4.4}$$

Therefore, 0 is not a solution of (4.2) and the trivial equilibrium $(0, 0)$ is not included in Theorem 4.1. In addition, in view of the proof in Appendix,

$$P\Big(1 - \frac{1}{r};\, r, v\Big) = (r - 1)(1 - v) < 0,$$

and $(1 - \frac{1}{r}, 0)$ is not an equilibrium. As a result, a nonnegative equilibrium of (2.2)–(2.3) would be either a positive feasible solution ($\mu^* > 0, s^* > 0$) or a trivial solution $(0, 0)$.

We now proceed to prove Theorem 4.1.

Proof. An equilibrium (μ^*, s^*) solves

$$\mu^* = F_1(\mu^*, s^*), \qquad s^* = F_2(\mu^*, s^*),$$

which can be written as

$$\mu^* = r(\mu^* - \mu^{*2} - s^*),$$

$$s^* = r^2v(\mu^{*4} - 2\mu^{*3} + \mu^{*2} + 6\mu^{*2}s^* - 6\mu^*s^* + s^* + 3s^{*2}) - r^2(\mu^* - \mu^{*2} - s^*)^2.$$

Now eliminating s^* from the first equation, we can solve for s^*:

$$\mu^*/r = \mu^* - \mu^{*2} - s^*,$$

and hence

$$s^* = \mu^* - \mu^{*2} - \frac{\mu^*}{r} = \mu^*\Big(1 - \frac{1}{r} - \mu^*\Big).$$

This expresses s^* as an explicit function of μ^*. Note immediately that for $s^* \geq 0$ we must have $1 - 1/r > 0$, and hence necessarily $r > 1$ for any nonnegative equilibrium; and furthermore

$$\mu^* \leq 1 - \frac{1}{r}$$

is required for feasibility.

Substituting into the second equilibrium equation, we first observe a useful simplification:

$$(\mu^* - \mu^{*2} - s^*)^2 = \frac{\mu^{*2}}{r^2}, \qquad r^2(\mu^* - \mu^{*2} - s^*)^2 = \mu^{*2}.$$

Now we have

$$s^* = r^2 v\, A(\mu^*, s^*) - \mu^{*2},$$

where

$$A(\mu, s) := \mu^4 - 2\mu^3 + \mu^2 + 6\mu^2 s - 6\mu s + s + 3s^2.$$

Substituting $s = \mu(1 - 1/r - \mu)$ into the polynomial $A(\mu, s)$, noting that

$$s = \mu\Big(1 - \frac{1}{r} - \mu\Big) = \mu - \frac{\mu}{r} - \mu^2, \tag{4.5}$$

$$s^2 = \mu^2\Big(1 - \frac{1}{r} - \mu\Big)^2 \tag{4.6}$$

$$= \mu^2\Big(1 - \frac{2}{r} + \frac{1}{r^2} - 2\mu + \frac{2\mu}{r} + \mu^2\Big) \tag{4.7}$$

$$= \mu^2 - \frac{2\mu^2}{r} + \frac{\mu^2}{r^2} - 2\mu^3 + \frac{2\mu^3}{r} + \mu^4, \tag{4.8}$$

we have

$$\begin{aligned} A(\mu, s) = {} & \\ & \mu^4 - 2\mu^3 + \mu^2 \\ & + \left(6\mu^3 - \frac{6\mu^3}{r} - 6\mu^4\right) \\ & + \left(-6\mu^2 + \frac{6\mu^2}{r} + 6\mu^3\right) \\ & + \left(\mu - \frac{\mu}{r} - \mu^2\right) \\ & + \left(3\mu^2 - \frac{6\mu^2}{r} + \frac{3\mu^2}{r^2} - 6\mu^3 + \frac{6\mu^3}{r} + 3\mu^4\right). \end{aligned} \tag{4.9}$$

A direct expansion (grouping powers of μ^*) yields

$$A(\mu^*, s^*) = -2\mu^{*4} + 4\mu^{*3} + (3(1/r^2 - 1))\mu^{*2} + \Big(1 - \frac{1}{r}\Big)\mu^*.$$

Note that

$$r^2 vA(\mu^*, s^*) = r^2 v\left(-2\mu^{*4} + 4\mu^{*3} - \frac{3(r^2-1)}{r^2}\mu^{*2} + \frac{r-1}{r}\mu^*\right)$$

$$= -2r^2 v\mu^{*4} + 4r^2 v\mu^{*3} - 3(r^2-1)v\mu^{*2} + (r-1)rv\mu^*.$$

Substituting the expression for $A(\mu^*, s^*)$ into $s^* = r^2 v\, A(\mu^*, s^*) - \mu^{*2}$, we have

$$s^* = -2r^2 v\mu^{*4} + 4r^2 v\mu^{*3} - 3(r^2-1)v\mu^{*2} + (r-1)rv\mu^* - \mu^{*2}.$$

In view of

$$s^* = \mu^*\left(\frac{r-1}{r} - \mu^*\right) = \frac{r-1}{r}\mu^* - \mu^{*2},$$

we have

$$\frac{r-1}{r}\mu^* - \mu^{*2} = -2r^2 v\mu^{*4} + 4r^2 v\mu^{*3} - 3(r^2-1)v\mu^{*2} + (r-1)rv\mu^* - \mu^{*2}.$$

Thus

$$2r^2 v\mu^{*4} - 4r^2 v\mu^{*3} + 3(r^2-1)v\mu^{*2} + \frac{(r-1)(1-r^2 v)}{r}\mu^* = 0.$$

Noting $\mu^* > 0$, we can divide the above equation by μ^* on both sides. Then multiplying through by r to clear the denominator $1/r$, one arrives at the cubic polynomial

$$2r^3 v\mu^{*3} - 4r^3 v\mu^{*2} + (3r^3 v - 3rv)\mu^* - r^3 v + r^2 v + r - 1 = 0,$$

which we denote by $P(\mu^*; r, v) = 0$. Therefore any positive equilibrium (μ^*, s^*) corresponds to a positive root μ^* of the cubic $P(\mu; r, v)$; and, conversely any real root μ^* of P with

$$0 < \mu^* \le 1 - \frac{1}{r}$$

gives a feasible equilibrium by taking $s^* = \mu^*(1 - 1/r - \mu^*)$ (which is then ≥ 0). Because P is a cubic in μ, it has at most three real roots; one of these may be $\mu^* = 0$ (the trivial root) and up to two further positive roots can lie inside the feasible interval $(0, 1 - 1/r]$. Thus for $r > 1$, the system can admit one or two positive biologically admissible equilibria (in addition to the trivial $(0, 0)$) depending on the parameters r and v. This completes the derivation and characterization of nontrivial equilibria. The proof that $P(\mu^*; r, v)$ has no feasible solutions for $r \ge 3$ is carried out in Section 5. □

The trivial equilibrium $(0, 0)$ always exists, but nontrivial equilibria appear when $r > 1$. For $r > 1$, Eqs (4.1)–(4.2) may admit up to two positive feasible roots $\mu_1^*, \mu_2^* \in (0, 1 - 1/r)$, corresponding to distinct stochastic steady states. For small v (close to 1), both equilibria lie near the deterministic logistic equilibrium $\mu^* \approx 1 - 1/r$.

4.2. Graphs of $P(\mu; r, v)$ and stability

Figures 2a–2c show the behavior of the cubic polynomial $P(\mu; r, v)$ for three representative parameter combinations. Each curve corresponds to the equilibrium condition $P(\mu^*; r, v) = 0$, whose roots determine the feasible nontrivial equilibrium means μ^* of the stochastic logistic model under the Gaussian moment closure. The shaded region indicates the biologically feasible interval $\mu \in (0, 1 - 1/r)$, within which positive equilibria are meaningful. For $r = 2.0$ and $v = 1.1$ (Figure 2a), the polynomial intersects the horizontal axis twice inside the feasible range, yielding two distinct nontrivial equilibria, one stable and one unstable. Similarly, for $r = 1.5$ and $v = 1.02$ (Figure 2b), two real roots also appear within the feasible region, but they occur at smaller μ values, indicating a lower equilibrium population level. For $r = 3$ and $v = 1.01$, Figure 2c shows there is no feasible solution. These results confirm that for $1 < r < 3$, system (4.1)–(4.2) may admit up to two positive feasible roots, and that there is no positive feasible solution for $r \geq 3$.

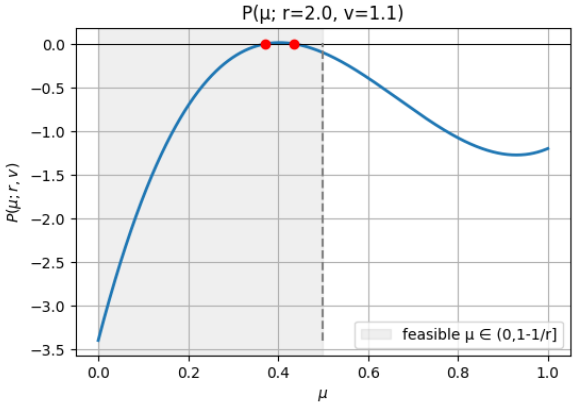

(a) P(μ;r,v) for $r = 2$, $v = 1.1$

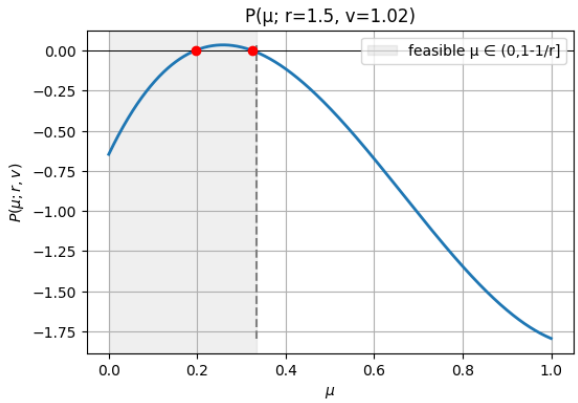

(b) P(μ;r,v) for $r = 1.5$, $v = 1.02$

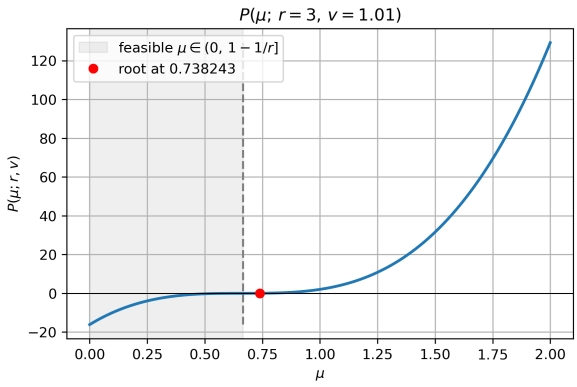

(c) P(μ;r,v) for $r = 3.1$, $v = 1.01$

Figure 2. Plots of P(μ;r,v).

For $r = 2.0$ and $v = 1.1$, as shown in Figure 2a, solving (4.2) gives three real roots:

$$\mu_1 \approx 0.37, \quad \mu_2 \approx 0.44, \quad \mu_3 \approx 1.19.$$

For $r = 2$, $s^* = \mu^*(\frac{1}{2} - \mu^*)$, and hence $s^* \geq 0$ requires $\mu^* \leq \frac{1}{2}$. Only μ_1 and μ_2 are within $(0, 0.5)$. Using (4.1),

$$s_1^* \approx 0.048, \qquad s_2^* \approx 0.028.$$

Linearization shows that (μ_2^*, s_2^*) is stable (all eigenvalues $|\lambda| < 1$), while (μ_1^*, s_1^*) is unstable. This pattern reflects a bistable structure typical in stochastic logistic systems: the lower equilibrium acts as a threshold separating extinction and persistence.

To determine local stability we linearize the moment system at an equilibrium (μ^*, s^*). The Jacobian of the moment map $(\mu, s) \mapsto (F_1(\mu, s), F_2(\mu, s))$ has the block form

$$J(\mu, s) = \begin{pmatrix} \partial_\mu F_1 & \partial_s F_1 \\ \partial_\mu F_2 & \partial_s F_2 \end{pmatrix} = \begin{pmatrix} r(1 - 2\mu) & -r \\ J_{21}(\mu, s) & J_{22}(\mu, s) \end{pmatrix},$$

where, with $r = 2$ and $v = 1.1$, the lower-left and lower-right entries are

$$J_{21}(\mu, s) = r^2 v(4\mu^3 - 6\mu^2 + 2\mu + 12\mu s - 6s) - r^2 \cdot 2(\mu - \mu^2 - s)(1 - 2\mu),$$
$$J_{22}(\mu, s) = r^2 v(6\mu^2 - 6\mu + 1 + 6s) - r^2 \cdot 2(\mu - \mu^2 - s)(-1).$$

Evaluating these expressions at the two feasible equilibria $\mu_1 \approx 0.371449$, $s_1 \approx 0.048$ and $\mu_2 \approx 0.436165$, $s_2 \approx 0.028$ yields the numerical Jacobians

$$J(\mu_1, s_1) \approx \begin{pmatrix} 0.514204 & -2.000000 \\ -0.177869 & 0.982669 \end{pmatrix}, \qquad J(\mu_2, s_2) \approx \begin{pmatrix} 0.255340 & -2.000000 \\ -0.040288 & 0.387282 \end{pmatrix}.$$

The eigenvalues of these matrices are

$$\operatorname{spec}(J(\mu_1, s_1)) \approx \{0.108,\ 1.389\}, \qquad \operatorname{spec}(J(\mu_2, s_2)) \approx \{0.030,\ 0.613\}.$$

Because one eigenvalue of $J(\mu_1, s_1)$ exceeds unity in modulus, (μ_1, s_1) is a saddle-type (locally unstable) equilibrium. By contrast both eigenvalues of $J(\mu_2, s_2)$ lie strictly inside the unit disk, so (μ_2, s_2) is locally asymptotically stable. Thus, for $r = 2.0$ and $v = 1.1$, the moment system has two feasible nontrivial equilibria. Trajectories near (μ_2, s_2) are attracted to the positive steady state, while (μ_1, s_1) forms an unstable threshold separating extinction-like behavior from persistence at the stable positive equilibrium.

Figure 3a plots the locations of the feasible equilibria μ^* as functions of v for $r = 2$, with the upper branch (orange) denoting the stable equilibrium and the lower branch (blue) the unstable one. The equilibrium equation $P(\mu^*; r, v) = 0$ was solved numerically to obtain all feasible equilibrium solutions, and the eigenvalues of the Jacobian matrix were computed to determine local stability. As v increases, the stable equilibrium μ^* gradually decreases, indicating that stronger environmental variability lowers the steady-state mean population level. Figure 3b shows the maximum eigenvalue modulus $|\lambda|$ of the stable equilibrium as a function of v, illustrating how increasing stochastic intensity pushes the eigenvalues toward the unit circle. When $|\lambda|$ approaches 1, the system reaches the stability boundary, and the equilibrium loses stability. Together, these results demonstrate that higher noise intensity reduces both population stability and equilibrium abundance, implying that environmental fluctuations can destabilize otherwise persistent populations by weakening the restoring forces around the equilibrium state.

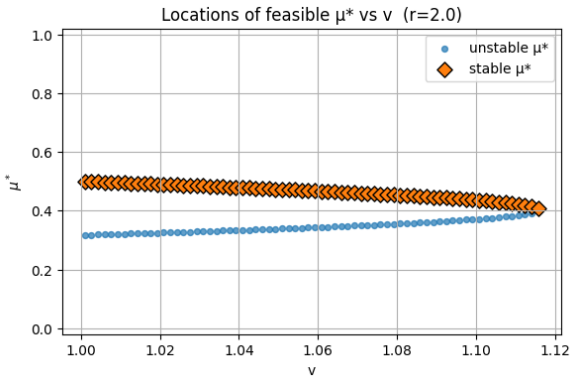

(a) μ vs v for $r = 2$

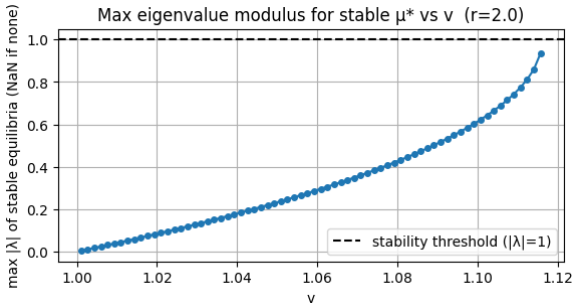

(b) Stability vs v for $r = 2$

Figure 3. Stability of nontrivial equilibria vs v.

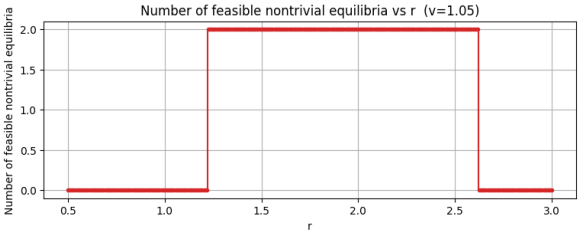

(a) Number of feasible nontrivial equilibria vs r

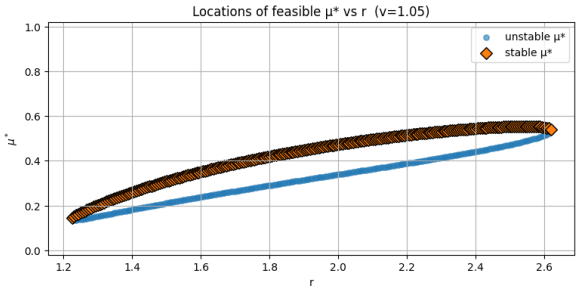

(b) Locations of feasible μ vs r

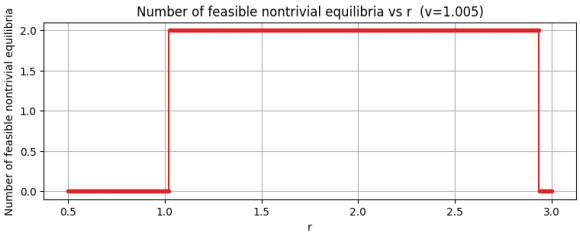

(c) Number of feasible nontrivial equilibria vs r

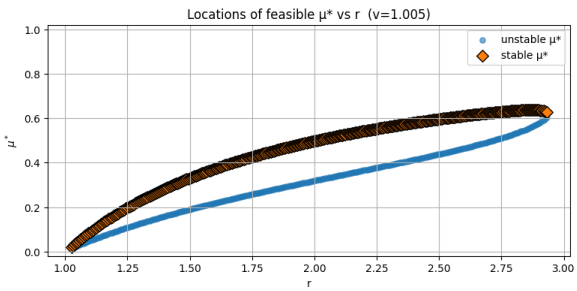

(d) Locations of feasible μ vs r

Figure 4. Stability of nontrivial equilibria vs r.

Figures 4a–4d illustrate the existence and stability of nontrivial equilibria for the stochastic logistic model as the intrinsic growth rate r varies. Figure 4 shows the number of feasible nontrivial equilibria (μ^*, s^*) identified from the analytic cubic equation $P(\mu^*; r, v) = 0$ for two values of the perturbation parameter v, while Figures 4b–4d display the corresponding equilibrium locations μ^* and their stability classification. Each equilibrium point is obtained by solving the moment system under Gaussian moment closure, with stability determined from the eigenvalues of the Jacobian matrix. In

the scatter plots, orange diamonds indicate the locally stable ones. These results were generated by sweeping r across the interval $[0.5, 3.0]$ and computing equilibrium solutions numerically for each value using the analytic formulas derived in this section.

The comparison between the two cases, $v = 1.05$ and $v = 1.005$, in Figure 4 demonstrates the impact of stochastic perturbation strength on equilibrium structure. For both values of v, nontrivial equilibria emerge when $r > 1$, consistent with the classical logistic bifurcation threshold. However, as the noise intensity increases (from $v = 1.005$ to $v = 1.05$), the feasible range of r supporting two nontrivial equilibria becomes slightly narrower, and the upper stable branch shifts downward. This indicates that stronger environmental variability reduces the region of parameter space where the population can sustain a positive stable mean level, effectively stabilizing the system around smaller equilibrium values. In other words, increasing stochastic fluctuations suppresses excessive growth and limits the persistence of large population states, a phenomenon commonly observed in noise-regularized dynamical systems.

4.3. Monte Carlo simulations

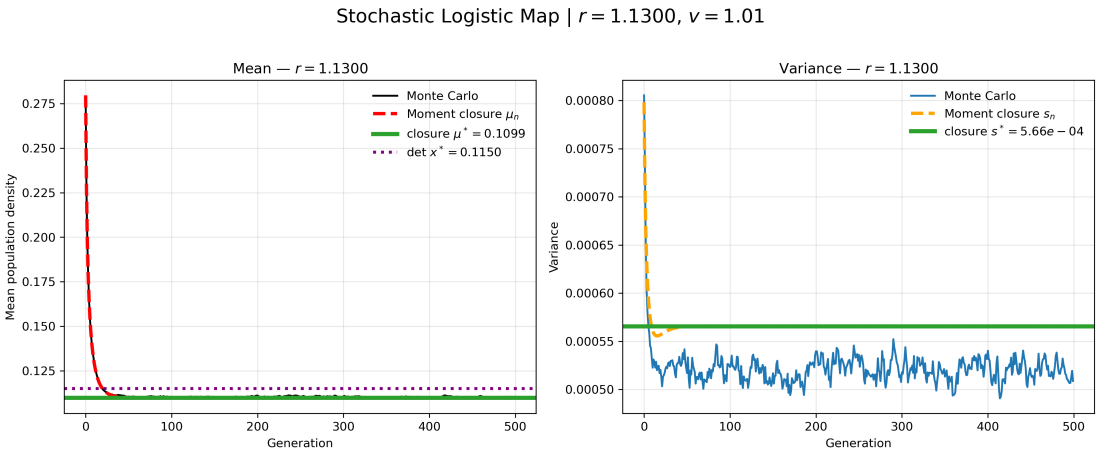

Figure 5. Monte Carlo simulation and Gaussian moment–closure predictions for $r = 1.13, v = 1.01$.

Figure 5 compares Monte Carlo simulations, the Gaussian moment–closure approximation, and the deterministic logistic fixed point for the stochastic logistic map at parameters $r = 1.13$ and $v = 1.01$. In the left panel, both the Monte Carlo mean trajectory (black curve) and the moment–closure mean μ_n (red dashed curve) rapidly converge to a small positive equilibrium. The horizontal green line marks the moment–closure fixed point $\mu^* \approx 0.1099$, while the purple dotted line shows the deterministic fixed point $x^* = 1 - \frac{1}{r} \approx 0.1150$. The two values are close, and the Monte Carlo mean settles between them, illustrating that the stochastic perturbations slightly depress the long–term population level relative to the deterministic prediction.

The right panel shows the corresponding variance dynamics. The Monte Carlo variance (blue curve) fluctuates around a small steady level, while the moment-closure variance s_n (orange dashed curve) relaxes quickly to the predicted equilibrium $s^* \approx 5.66 \times 10^{-4}$ (green line). The agreement is again excellent, with the closure equations capturing both the magnitude and transient behavior of variance.

Overall, the figure demonstrates that for moderate growth rates $1 < r < 3$ and weak noise ($v \approx 1$), the Gaussian moment–closure system accurately tracks the Monte Carlo dynamics in both mean and variance, while deviating slightly from the deterministic logistic equilibrium due to stochastic effects.

Biologically, the stability of a nontrivial equilibrium (μ^*, s^*) represents the long-term persistence of a population at a positive mean abundance under stochastic environmental fluctuations. When the nontrivial equilibrium is locally asymptotically stable, the population converges toward a steady-state level μ^* after transient fluctuations, indicating a balance between intrinsic growth, density-dependent regulation, and random environmental effects.

In this regime, the variance s^* quantifies the expected amplitude of natural population fluctuations around the mean equilibrium, reflecting environmental variability. The parameter condition $r > 1$ ensures the existence of positive equilibria, while increasing stochastic intensity v can reduce stability by narrowing the feasible range of r and lowering the equilibrium population size. Thus, stability of the nontrivial equilibrium signifies ecological resilience—the capacity of the population to maintain a sustainable level despite environmental randomness—whereas loss of stability marks the onset of stochastic instability and heightened extinction risk.

4.4. Bifurcation analysis

System (2.2)–(2.3) is a two–dimensional map driven by two parameters (r, v), unlike the one–dimensional deterministic model depending only on r, and its bifurcation structure may be substantially richer. In this study, however, we focus on the saddle-node (fold) bifurcation with respect to the stochastic intensity v because it represents the primary mechanism through which environmental variability alters the qualitative behavior of the system, leading to the coalescence and disappearance of positive equilibria. This type of bifurcation is consistent with the canonical one-dimensional fold, where two equilibria (one stable and one unstable) merge as a control parameter varies, producing a qualitative transition from persistence to extinction in the underlying dynamical process [20, 21].

Theorem 4.3 (Saddle-node bifurcation)**.** *Under the assumptions of Theorem 2.1, and assume that* $r > 1$*, the saddle-node bifurcation of* (2.2)–(2.3) *occurs at a critical noise level* $v = v_c$ *at*

$$v_c(r) = -\frac{r-1}{2r^3(\mu_c)^3 - 4r^3(\mu_c)^2 + (3r^3 - 3r)\mu_c - r^3 + r^2} \tag{4.10}$$

where $\mu_c(r) = \frac{4r - \sqrt{2(9-r^2)}}{6r}$ *for* $1 < r < 3$.

Proof. The saddle-node bifurcation occurs at a critical noise level $v = v_c$ where the equilibrium equation $P(\mu^*; r, v) = 0$ and its derivative with respect to μ^* vanish simultaneously, that is,

$$P(\mu^*; r, v_c) = 0, \qquad \frac{\partial P}{\partial \mu^*}(\mu^*; r, v_c) = 0.$$

At this bifurcation point, the two real roots of $P(\mu^*; r, v)$ coalesce into a single double root, corresponding to a marginally stable equilibrium. For $v < v_c$, two distinct equilibria exist—one stable and one unstable—whereas for $v > v_c$, no feasible positive equilibrium persists. This analytic condition precisely characterizes the threshold at which increasing environmental variability eliminates the population's stable steady state.

Recall that

$$P(\mu; r, v) = 2r^3v\mu^3 - 4r^3v\mu^2 + (3r^3v - 3rv)\mu - r^3v + r^2v + r - 1.$$

Differentiating P with respect to μ gives

$$\frac{\partial P}{\partial \mu} = 6r^3v\mu^2 - 8r^3v\mu + (3r^3v - 3rv).$$

Factor v (we are interested in $v > 0$):

$$\frac{\partial P}{\partial \mu} = v(6r^3\mu^2 - 8r^3\mu + 3r^3 - 3r) \equiv v\ Q(\mu; r).$$

Thus for $v > 0$ the saddle–node condition $\partial_\mu P = 0$ reduces to the quadratic

$$Q(\mu; r) \ = \ 6r^3\mu^2 - 8r^3\mu + 3r^3 - 3r \ = \ 0.$$

Solving $6r^3\mu^2 - 8r^3\mu + 3r^3 - 3r = 0$ gives

$$\mu \ = \ \frac{8r^3 \pm \sqrt{(8r^3)^2 - 4(6r^3)(3r^3 - 3r)}}{12r^3}.$$

The discriminant simplifies algebraically:

$$(8r^3)^2 - 4(6r^3)(3r^3 - 3r) = 64r^6 - 24r^3(3r^3 - 3r) \tag{4.11}$$
$$= 64r^6 - 72r^6 + 72r^4 \tag{4.12}$$
$$= 8r^4(9 - r^2). \tag{4.13}$$

Substituting and simplifying yields the two candidate roots:

$$\mu_c^{\pm}(r) = \frac{4r \pm \sqrt{2}\ \sqrt{9 - r^2}}{6r} \ = \ \frac{4r \pm \sqrt{2(9 - r^2)}}{6r}$$

These are real only when $9 - r^2 \geq 0$, i.e., $r \leq 3$. The polynomial P is affine (linear) in v; we write it as

$$P(\mu; r, v) = v \cdot B(\mu; r) + (r - 1),$$

where

$$B(\mu; r) = 2r^3\mu^3 - 4r^3\mu^2 + (3r^3 - 3r)\mu - r^3 + r^2.$$

Solving $P(\mu; r, v) = 0$ for v gives

$$v \ = \ -\frac{r - 1}{B(\mu; r)}.$$

The saddle–node candidates are obtained by evaluating the formula for v at $\mu = \mu_c^{\pm}(r)$.

As shown in Figure 6, we only need $\mu_c^-(r)$ because of $0 < \mu \leq 1 - 1/r$ (equivalently $s^* \geq 0$). These are real only when $9 - r^2 \geq 0$, i.e., $r \leq 3$. The saddle–node candidates are obtained by evaluating the formula for v at $\mu = \mu_c^-(r)$. Thus

$$v_c^-(r) \ = \ -\frac{r - 1}{B(\mu_c^-(r),\ r)}$$

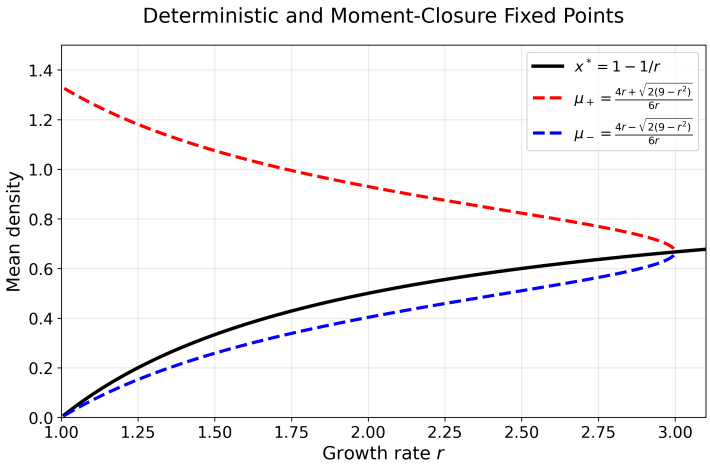

Figure 6. Deterministic and moment-closure fixed points.

where $B(\mu; r)$ is the cubic coefficient function above and

$$\mu_c^-(r) = \frac{4r \pm \sqrt{2(9-r^2)}}{6r}, \qquad (r \le 3).$$

As a result, the analytic candidate locations of fold points (μ_c, v_c) are

$$\mu_c(r) = \frac{4r - \sqrt{2(9-r^2)}}{6r} \tag{4.14}$$

$$v_c(r) = -\frac{r-1}{2r^3(\mu_c)^3 - 4r^3(\mu_c)^2 + (3r^3 - 3r)\mu_c - r^3 + r^2}. \tag{4.15}$$

□

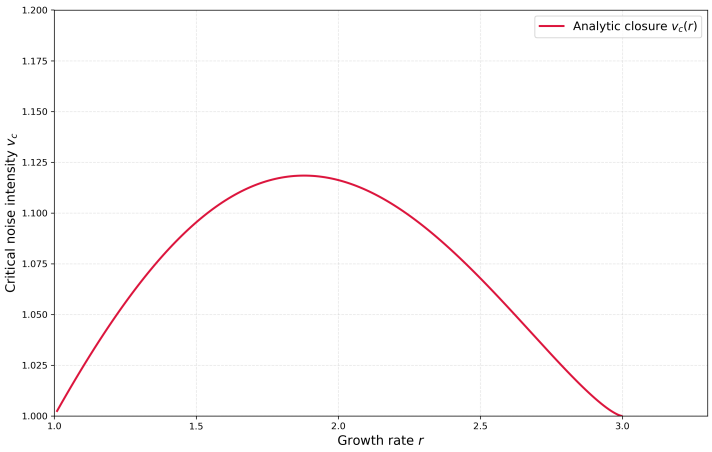

Figure 7. Fold (saddle-node) bifurcation curve $v_c(r)$.

We now look at the representative case $r = 2$. To investigate the influence of stochastic intensity v on the stability of the nontrivial equilibrium, numerical simulations were performed for a fixed intrinsic

growth rate $r = 2.0$ while varying v incrementally above 1. For the prototypical case $r = 2$, the bifurcation threshold v_c is found by imposing the saddle-node (fold) conditions on the equilibrium polynomial $P(\mu^*; r, v)$:

$$P(\mu^*; 2, v) = 0, \qquad \frac{\partial P}{\partial \mu^*}(\mu^*; 2, v) = 0.$$

Substituting $r = 2$ into (4.2) gives

$$P(\mu; 2, v) = 16v\mu^3 - 32v\mu^2 + 18v\mu - 4v + 1.$$

The saddle–node conditions are

$$P(\mu; 2, v) = 0, \qquad \frac{\partial P}{\partial \mu}(\mu; 2, v) = 0.$$

Differentiating gives

$$P'(\mu; 2, v) = 48v\mu^2 - 64v\mu + 18v.$$

Since $v > 1$, the equation $P'(\mu; 2, v) = 0$ reduces to the quadratic

$$48\mu^2 - 64\mu + 18 = 0 \quad \Longleftrightarrow \quad 24\mu^2 - 32\mu + 9 = 0.$$

Solving this quadratic yields the two exact roots

$$\mu = \frac{2}{3} \pm \frac{\sqrt{10}}{12}.$$

Thus

$$\mu_1 = \frac{2}{3} - \frac{\sqrt{10}}{12} \approx 0.4031435283, \qquad \mu_2 = \frac{2}{3} + \frac{\sqrt{10}}{12} \approx 0.9301898050.$$

To obtain the corresponding v values, substitute either root into $P(\mu; 2, v) = 0$ and solve for v. This gives the closed-form values

$$v_1 = \frac{8 + \sqrt{10}}{10} \approx 1.1162277660, \qquad v_2 = \frac{8 - \sqrt{10}}{10} \approx 0.4837722340.$$

Recall the equilibrium relation

$$s^* = \mu^*\Big(1 - \frac{1}{r} - \mu^*\Big).$$

For $r = 2$, this becomes $s^* = \mu^*(\frac{1}{2} - \mu^*)$, hence physical admissibility of the equilibrium (nonnegative s^*) requires $\mu^* \le \frac{1}{2}$. Of the two algebraic roots above only $\mu_1 \approx 0.40314$ satisfies this constraint; the root $\mu_2 \approx 0.93019$ yields $s^* < 0$ and is therefore not admissible. The relevant saddle–node (fold) for $r = 2$ is

$$\mu_c \approx 0.4031435283, \qquad v_c \approx 1.1162277660.$$

The fold curve $v_c(r)$ in Figure 7 first increases with r and then decreases until $r \approx 3$. For small values of $r > 1$, population growth is weak and even moderate noise destroys the positive equilibrium, resulting in small v_c. As r increases, the intrinsic growth rate strengthens the system's resilience to stochastic fluctuations, allowing larger noise intensities before the stable and unstable equilibria

coalesce; consequently, $v_c(r)$ rises and reaches its maximum near $r \approx 1.8$. However, when r becomes large ($r > 3$), the deterministic logistic map itself loses stability through period-doubling bifurcations [2], and the cubic equilibrium equation $P(\mu; r, v) = 0$ no longer possesses two real feasible roots. Thus, the fold bifurcation disappears.

Biologically, the fold bifurcation represents a critical threshold of environmental noise intensity: as stochastic variability increases beyond the bifurcation point v_c, the population loses its stable positive equilibrium and is driven toward extinction or large fluctuations. Thus, the saddle-node bifurcation in v quantifies how increasing environmental noise undermines population stability, providing a mechanistic explanation for noise-induced collapse in stochastic logistic systems. Biologically, this means that populations with moderate intrinsic growth rates are most robust to environmental variability, whereas those with very small or very large r values are more susceptible to noise-induced extinction.

5. Conclusions and discussion

This study develops a moment-based analytical framework for understanding the dynamics of stochastic logistic population models. Under the Gaussian moment-closure approximation, by deriving a system of difference equations for the first and second moments directly from the stochastic logistic equation, we establish a unified approach to study population persistence and extinction under environmental variability. The stability analysis reveals two qualitatively distinct equilibria: a trivial equilibrium corresponding to extinction and one or two nontrivial equilibria representing sustainable population levels. The condition $r^2 v < 1$ ensures the stability of the extinction state, while $r > 1$ leads to the emergence of positive equilibria whose stability depends on the stochastic intensity $v = E[\varepsilon_n^2]$.

We analyzed the saddle-node (fold) bifurcation that arises as the stochastic intensity v varies, illustrating how increasing noise intensity leads to the merging and disappearance of stable and unstable equilibria. These results provide theoretical and biological insights into how the balance between intrinsic growth and environmental variability governs long-term population stability, resilience, and extinction risk. Numerical simulations were carried out to illustrate the theoretical predictions of the moment-based stability analysis and to visualize the dependence of the equilibrium structure on the parameters r and v. By numerically solving the equilibrium condition $P(\mu^*; r, v) = 0$ across a range of r values for fixed v, we identified two feasible nontrivial equilibria within the interval $(0, 1 - 1/r)$ and determined their stability through the eigenvalues of the Jacobian matrix. The simulation results revealed a clear bistable structure: an upper stable branch and a lower unstable branch that merge at a critical value of v, beyond which no positive equilibrium exists. These numerical results confirmed the analytical predictions based on the saddle-node bifurcation result, showing excellent agreement between the theoretical stability boundaries and the computed equilibrium curves.

To further validate the analytical and numerical findings, Monte Carlo simulations were performed by generating large ensembles of stochastic trajectories based on the recurrence relation $X_{n+1} = rX_n(1 - X_n)\varepsilon_n$, where ε_n are independent lognormal perturbations with $E[\varepsilon_n] = 1$ and $E[\varepsilon_n^2] = v$. The ensemble mean and variance of X_n were tracked over time and compared with the theoretical moment-map predictions.

The Monte Carlo simulations consistently confirmed the validity of the Gaussian moment–closure

approximation across the full range of parameter values examined. In the regime $0 < r < 1$, both the deterministic and stochastic models predict extinction, and the simulations showed rapid convergence of the sample mean and variance to the trivial equilibrium $(\mu^*, s^*) = (0, 0)$, in precise agreement with the moment–closure dynamics. For $1 < r < 3$, where the moment-map analysis identifies a single stable nontrivial equilibrium, the ensemble average of X_n approached the predicted mean μ^*, while the sample variance settled near the corresponding s^*, thereby confirming the local stability inferred from the Jacobian eigenvalue analysis. When both the intrinsic growth rate r and noise intensity v remained close to unity, the Monte Carlo trajectories stabilized rapidly and exhibited nearly Gaussian fluctuations around equilibrium. This behavior reflects the regularizing influence of weak multiplicative noise, which tends to suppress the nonlinear distortions characteristic of the deterministic logistic map and maintain an approximately normal distribution of population states. Overall, the Monte Carlo results validate the theoretical assumptions underlying the Gaussian moment closure and provide strong numerical support for the analytic conclusions regarding extinction, equilibrium existence, and local stability.

The nonexistence of biologically feasible solutions of $P(\mu; r, v) = 0$ for $r \geq 3$ stands in clear *contrast* to the deterministic logistic map, where the first flip (period–doubling) bifurcation occurs precisely at $r = 3$, when the positive fixed point $x^* = 1 - \frac{1}{r}$ loses stability and a period–two orbit is created [2]. This is consistent with the saddle-node bifurcation boundary at $r = 3$ in Theorem 4.3. Since no feasible equilibrium exists for the moment equations when $r \geq 3$, a flip bifurcation cannot occur in this region of parameter space, and the classical period–doubling cascade of the deterministic logistic map has no direct analogue in the present closure framework.

It is also important to note that the moment system is a two–dimensional map driven by two parameters (r, v), unlike the one-dimensional deterministic model depending only on r. Consequently, its bifurcation structure may be substantially richer, potentially including higher–dimensional phenomena that have no deterministic counterpart. However, the present paper focuses specifically on saddle-node bifurcations with respect to the noise-intensity parameter v, as our primary goal is to understand how varying the level of multiplicative stochasticity affects the emergence and disappearance of equilibria. A systematic exploration of other possible bifurcations in the (r, v) parameter plane is beyond the scope of this work and will be examined in future studies.

In addition, it is worth emphasizing that the nonnegativity of the population mean is not automatically guaranteed by the Gaussian moment-closure approximation. Even if the process begins with a nonnegative mean, the update rule for the next-step mean does not, on its own, ensure that subsequent values will always remain biologically feasible. This is precisely where the structure imposed by moment-closure theory becomes essential. The moment-closure framework provides the consistency conditions needed to keep the first moment in a biological feasibility region, even though the normal approximation itself assigns probability to negative values. Thus, even though the Gaussian approximation assigns a small probability to negative population values, the closed system of moment equations restricts attention to the dynamics of the *mean*, which remains nonnegative throughout the iteration. In this sense, the Gaussian moment closure preserves a form of nonnegativity appropriate for deterministic descriptions of expected population behavior: the population mean never becomes negative, and the variance, by definition, is nonnegative as well. This allows the approximation to remain biologically interpretable at the level of (μ_n, s_n), even though the normal distribution assumed for closure extends over the entire real line.

The limitations of the Gaussian moment-closure approximation become most apparent when viewed across different growth-rate regimes. When $r < 1$, both the Monte Carlo simulations and the moment equations predict rapid convergence to the extinction state, and the approximation performs exceptionally well because stochastic fluctuations remain small and the trajectories remain close to zero. For $1 < r < 3$, where the deterministic logistic map retains a single stable fixed point, the moment closure continues to provide reasonably accurate predictions: Monte Carlo simulations show that the sample paths fluctuate around a well-defined positive level, and the mean and variance predicted by the closure closely match those observed in simulation. However, as r approaches the bifurcation threshold near $r = 3$, the situation changes markedly. As shown above, the cubic equilibrium condition $P(\mu; r, v) = 0$ has *no feasible positive root* in Theorem 4.1 whenever $r \geq 3$, which means that the moment-closure system does not admit a biologically meaningful equilibrium in the very region where the deterministic logistic map undergoes its first flip bifurcation.

These observations underscore an important structural difference between the deterministic and moment-closure descriptions. Whereas the deterministic map develops increasingly complicated dynamics beyond $r = 3$, the moment equations lose their equilibrium structure and are no longer reliable as a reduced representation of the stochastic process. Thus, the Gaussian closure should be regarded as an accurate and practical approximation primarily within the range $1 < r < 3$, where Monte Carlo simulations confirm its predictions for both mean and variance. Beyond this regime, especially near bifurcation boundaries, and more refined closure schemes may be required to capture the full range of noise-induced phenomena. Developing and analyzing such improved closures is a natural direction for future work.

The theoretical framework developed in this study can be directly applied to the analysis of real ecological or biological population data. By estimating the intrinsic growth rate r, the stochastic intensity $v = E[\varepsilon_n^2]$, and the empirical moments $E[X_n]$ and $\mathrm{Var}[X_n]$ from observed time-series data, the derived system of moment equations can be used to evaluate the stability properties of the underlying population. Fitting the stochastic logistic model to data allows researchers to identify whether the population operates near a stable nontrivial equilibrium or within a parameter regime that leads to extinction or strong fluctuations. In practice, parameters can be estimated using regression or likelihood-based techniques, and Monte Carlo simulations can then be employed to assess how environmental noise affects the predicted population trajectories. This integration of theory and data provides a powerful tool for predicting long-term population behavior under variable environmental conditions, assessing extinction risk, and evaluating the potential effects of management or conservation strategies on population persistence.

Use of AI tools declaration

The authors declare they have not used Artificial Intelligence (AI) tools in the creation of this article.

Acknowledgments

HW dedicates this work to his colleague and friend, Professor Yang Kuang, on the occasion of his 60th birthday. The authors would like to thank the reviewers for their constructive comments that helped improve the paper.

Conflict of interest

Haiyan Wang is an editorial board member for Mathematical Biosciences and Engineering and was not involved in the editorial review or the decision to publish this article. All authors declare that there are no competing interests.

References

1. J. D. Murray, *Mathematical Biology I: An Introduction*, Springer, 2002.
2. R. M. May, Simple mathematical models with very complicated dynamics, *Nature*, **261** (1976), 459–467. https://doi.org/10.1038/261459a0
3. M. Kot, *Elements of Mathematical Ecology*, Cambridge University Press, 2001.
4. M. Aktar, U. Karim, V. Aithal, A. R. Bhowmick, Random variation in model parameters: A comprehensive review of stochastic logistic growth equation, *Ecol. Modell.*, **484** (2023), 110475. https://doi.org/10.1016/j.ecolmodel.2023.110475
5. L. J. S. Allen, *An Introduction to Stochastic Processes with Applications to Biology*, Chapman and Hall/CRC, 2010.
6. S. J. Schreiber, S. Huang, J. Jiang, H. Wang, Extinction and quasi-stationarity for discrete-time, endemic SIS and SIR models, *SIAM J. Appl. Math.*, **81** (2021), 2195–2217. https://doi.org/10.1137/20M1339015
7. E. Braverman, A. Rodkina, Difference equations of Ricker and logistic types under bounded stochastic perturbations with positive mean, *Comput. Math. Appl.*, **66** (2013), 2281–2294. https://doi.org/10.1016/j.camwa.2013.06.014
8. Y. Kang, P. Chesson, Relative nonlinearity and permanence, *Theor. Popul. Biol.*, **78** (2010), 26–35. https://doi.org/10.1016/j.tpb.2010.04.002
9. H. Makarem, H. N. Pishkenari, G. R. Vossoughi, A modified Gaussian moment closure method for nonlinear stochastic differential equations, *Nonlinear Dyn.*, **89** (2017), 2609–2620. https://doi.org/10.1007/s11071-017-3608-9
10. L. Marrec, C. Bank, T. Bertrand, Solving the stochastic dynamics of population growth, *Ecol. Evol.*, **13** (2023), e10295. https://doi.org/10.1002/ece3.10295
11. J. H. Matis, T. R. Kiffe, On approximating the moments of the equilibrium distribution of a stochastic logistic model, *Biometrics*, **52** (1996), 980–991. https://doi.org/10.2307/2533059
12. L. Socha, Moment equations for nonlinear stochastic dynamic systems (NSDS), in *Linearization Methods for Stochastic Dynamic Systems*, Springer, (2008), 85–102. https://doi.org/10.1007/978-3-540-72997-6_4
13. H. Wang, A. Tsiairis, J. Duan, Bifurcation in mean phase portraits for stochastic dynamical systems with multiplicative gaussian noise, *Int. J. Bifurcation Chaos*, **30** (2020), 2050216. https://doi.org/10.1142/S0218127420502168
14. H. Wang, Equilibrium analysis of discrete stochastic population models with gamma distribution, *Math. Biosci.*, **381** (2025), 109398. https://doi.org/10.1016/j.mbs.2025.109398

15. H. Wang, Analysis of discrete stochastic population models with normal distribution, preprint, arXiv:2504.14296. https://doi.org/10.48550/arXiv.2504.14296

16. H. Wang, Y. Wang, Detecting transitions from steady states to chaos with gamma distribution, *Int. J. Bifurcation Chaos*, **35** (2025), 2550163. https://doi.org/10.1142/S0218127425501639

17. E. Lakatos, A. Ale, P. D. Kirk, M. P. Stumpf, Multivariate moment closure techniques for stochastic kinetic models, *J. Chem. Phys.*, **143** (2015), 094107. https://doi.org/10.1063/1.4929837

18. Wikipedia Contributors, Normal distribution, *Wikipedia, The Free Encyclopedia*, 2024. Available from: https://en.wikipedia.org/wiki/Normal_distribution.

19. S. N. Elaydi, *An Introduction to Difference Equations*, 3rd edition, Springer, New York, 2005.

20. Y. A. Kuznetsov, *Elements of Applied Bifurcation Theory*, 3rd edition, Springer-Verlag, New York, 2004.

21. J. M. Grandmont, Nonlinear difference equations, bifurcations and chaos: An introduction, *Res. in Econ.*, **62** (2008), 122–177. https://doi.org/10.1016/j.rie.2008.06.003

Appendix

In this section, we prove that the claim in Theorem 4.1 that $P(\mu; r, v) = 0$ has no feasible solution for $r \geq 3$.

Proof. Fix $r > 1$ and $v > 1$. Recall that a nontrivial equilibrium must satisfy $P(\mu; r, v) = 0$ for some μ in the feasible interval

$$\mathcal{I}_r = \Big[0,\ 1 - \frac{1}{r}\Big],$$

with the associated variance $s^* = \mu(1 - \frac{1}{r} - \mu) \geq 0$. We show that when $r \geq 3$, the cubic $P(\mu; r, v)$ is strictly negative on $\mathcal{I}_r$ and therefore admits no feasible root. Evaluate P at $\mu = 0$:

$$P(0; r, v) = -r^3 v + r^2 v + r - 1 = (r - 1)(1 - r^2 v).$$

Since $r > 1$ and $v > 1$, we have $r^2 v \geq r^2 > 1$, and therefore

$$P(0; r, v) < 0.$$

Next evaluate P at the upper boundary $\mu = 1 - \frac{1}{r}$.

$$\begin{aligned}
P\Big(1 - \frac{1}{r};\, r, v\Big) &= 2r^3 v\Big(1 - \frac{1}{r}\Big)^3 - 4r^3 v\Big(1 - \frac{1}{r}\Big)^2 + (3r^3 v - 3rv)\Big(1 - \frac{1}{r}\Big) - r^3 v + r^2 v + r - 1 \\
&= 2r^3 v\Big(1 - \frac{3}{r} + \frac{3}{r^2} - \frac{1}{r^3}\Big) - 4r^3 v\Big(1 - \frac{2}{r} + \frac{1}{r^2}\Big) \\
&\quad + (3r^3 v - 3rv)\Big(1 - \frac{1}{r}\Big) - r^3 v + r^2 v + r - 1 \\
&= (2r^3 v - 6r^2 v + 6rv - 2v) + (-4r^3 v + 8r^2 v - 4rv) \\
&\quad + (3r^3 v - 3r^2 v - 3rv + 3v) - r^3 v + r^2 v + r - 1 \\
&= (2 - 4 + 3 - 1)r^3 v + (-6 + 8 - 3 + 1)r^2 v \\
&\quad + (6 - 4 - 3)rv + (-2 + 3)v + r - 1 \\
&= 0 \cdot r^3 v + 0 \cdot r^2 v - rv + v + r - 1 \\
&= (r - 1) - v(r - 1) \\
&= (r - 1)(1 - v).
\end{aligned}$$

For $v > 1$, this quantity is strictly negative. Thus,

$$P\Big(1 - \tfrac{1}{r};\, r, v\Big) < 0 \qquad \text{for all } r > 1,\ v > 1.$$

Differentiate P with respect to μ:

$$P_\mu(\mu; r, v) = 6r^3 v\,\mu^2 - 8r^3 v\,\mu + (3r^3 v - 3rv).$$

Factor $rv > 0$ to obtain

$$P_\mu(\mu; r, v) = rv\Big(6r^2\mu^2 - 8r^2\mu + 3r^2 - 3\Big).$$

Define the quadratic

$$q(\mu) = 6\mu^2 - 8\mu + 3.$$

Its discriminant is $(-8)^2 - 4 \cdot 6 \cdot 3 = -8 < 0$, so $q(\mu) > 0$ for all $\mu \in \mathbb{R}$. The minimum occurs at $\mu = 2/3$ and $q_{\min} = q(2/3) = 1/3$. Thus

$$6\mu^2 - 8\mu + 3 \ \geq\ \frac{1}{3} \qquad \text{for all } \mu \in \mathbb{R}.$$

Using this lower bound,

$$P_\mu(\mu; r, v) \geq rv\Big(r^2 \cdot \tfrac{1}{3} - 3\Big) = rv \cdot \frac{r^2 - 9}{3}.$$

Therefore, if $r \geq 3$, then $r^2 - 9 \geq 0$ and

$$P_\mu(\mu; r, v) \geq 0 \qquad \text{for all } \mu \in \mathcal{I}_r.$$

Hence $P(\mu; r, v)$ is nondecreasing on the entire feasible interval.

Since $P(\mu)$ is nondecreasing on $\mathcal{I}_r$ and negative at both endpoints, it must satisfy

$$P(\mu; r, v) < 0 \qquad \text{for every } \mu \in \mathcal{I}_r.$$

Thus $P(\mu; r, v)$ cannot vanish on $\mathcal{I}_r$ when $r \geq 3$ and $v \geq 1$. Hence no biologically feasible nontrivial equilibrium exists in this range. This proves that the moment-closure system admits no positive solution (μ^*, s^*) for $r \geq 3$, establishing the claim. □

AIMS Press